Title: Experimental infection of tick cells with Nipah virus

Phoon, W.H. [1], Bell-Sakyi, L. [2], AbuBakar, S. [3] and Chang, L.Y. [1,*]

[1] Department of Medical Microbiology, Universiti Malaya, 50603 Kuala Lumpur, Malaysia

[2] Institute of Infection, Veterinary and Ecological Science, University of Liverpool, 146 Brownlow Hill, Liverpool L3 5RF, United Kingdom

[3] Tropical Infectious Diseases Research & Education Centre, Universiti Malaya, 50603 Kuala Lumpur, Malaysia

* Corresponding author: changliyen@um.edu.my

ABSTRACT

Nipah virus (NiV), a highly pathogenic henipavirus of the family *Paramyxoviridae*, which causes fatal encephalitis in 40-70% of affected patients, was first reported in Malaysia over 20 years ago. Pteropid bats are the natural hosts of henipaviruses, and ticks have been proposed as a possible link between bats and mammalian hosts. To investigate this hypothesis, infection of the tick cell line IDE8 with NiV was examined. Presence of viral RNA and antigen in the NiV-infected tick cells was confirmed. Infectious virions were recovered from NiV-infected tick cells and ultrastructural features of NiV were observed by electron microscopy. These results suggest that ticks could support NiV infection, potentially playing a role in transmission.

KEYWORDS: henipavirus infection, Chiroptera, ticks, viral RNA, electron microscopy

INTRODUCTION

Nipah virus (NiV), a member of the family *Paramyxoviridae*, was first identified in 1998 in Malaysia as the causative agent of an outbreak of febrile encephalitis in patients associated with pig farming (Chua *et al.*, 2000). Since then, multiple disease outbreaks involving NiV have been reported almost annually in Bangladesh (Hsu *et al.*, 2004; Luby *et al.*, 2009), while isolated outbreaks occurred in India (Chadha *et al.*, 2006; Arunkumar *et al.*, 2019; Yadav *et al.*, 2022) and the Philippines (Ching *et al.*, 2015). Serological and virological analyses have provided evidence to support pteropid fruit bats as the likely reservoir of NiV (Field *et al.*, 2001; Yob *et al.*, 2001; Chua, 2003). In Malaysia, NiV transmission from reservoir host to susceptible animals was believed to occur through exposure to bat excreta or saliva in fruits that were partially eaten by bats (Chua *et al.*, 2002; Rahman *et al.*, 2010). Humans then

contracted the infection through close contact with NiV-infected pigs, specifically direct contact with body fluids or secretions of the infected pigs (Amal *et al.*, 2000; Parashar *et al.*, 2000). Molecular evidence of identical sequences from the NiV strains isolated from diseased pigs and humans confirmed the direct transmission of NiV from pigs to humans (AbuBakar *et al.*, 2004). On the other hand, ticks have been proposed as a potential vector of a close relative of NiV, the Hendra virus (HeV), from bats to horses and other mammals (Barker, 2003). Generally, ticks are blood-feeding parasites that harbour various microorganisms and infectious pathogens, including arboviruses such as Crimean-Congo haemorrhagic fever virus and tick-borne encephalitis virus (Nicholson *et al.*, 2018). Tick cell lines are known to support the replication of a wide range of arboviruses as well as viruses with no known arthropod vectors, including arenaviruses (Bell-Sakyi *et al.*, 2012; Hepojoki *et al.*, 2015). However, to date, there is no report available on paramyxovirus infection of tick cells. Considering that ticks could be the interface between bats and livestock and humans, this study aimed to investigate the ability of tick cells to support NiV infection.

MATERIALS AND METHODS

Virus and cells

The NiV Sungai Buloh strain/NiV/MY/99/VRI-2794 (AbuBakar *et al.*, 2004), was propagated in Vero cells (CCL-81) (ATCC, USA) and maintained in Gibco™ Minimum Essential Medium with Earle's salts (EMEM) (Thermo Fisher Scientific, USA) supplemented with 2% fetal bovine serum (FBS), 2 mM L-glutamine and 1% non-essential amino acids at 37°C with 5% CO_2. The IDE8 tick cell line, derived from embryonated eggs of the black-legged tick *Ixodes scapularis* (Munderloh *et al.*, 1994) was maintained in Nunc™ flat-sided tubes (Thermo Fisher Scientific, USA) in Gibco™ Leibovitz's L-15 medium (Thermo Fisher

Scientific, USA) prepared with some modifications (Munderloh & Kurtti, 1989). The modified L-15 medium (L-15B) contained 5% FBS, 10% tryptose phosphate broth, 0.1% bovine lipoprotein concentrate (MP Biomedicals, Thermo Fisher Scientific, USA), 2 mM L-glutamine, 100 units/ml penicillin and 100 µg/mL streptomycin. The IDE8 cells were incubated in ambient air at 28°C with medium changed weekly, and subcultured when necessary.

All experiments involving the use of live NiV were performed at the biosafety level 3 (BSL3) facility in Universiti Malaya (UM). NiV is classified as a risk group 3 agent in Malaysia under the Prevention and Control of Infectious Diseases Act 1998, Malaysia, and biorisk assessment was performed and approved by the UM Institutional Biosafety and Biosecurity Committee.

Preparation of NiV inoculum

Purified NiV stock (100 µL) was added to Vero cells at 80% confluency, and pre-absorbed for 1 h at 37°C, followed by rinsing with serum-free medium to remove unbound virus. NiV-infected Vero cells were incubated at 37°C. When 90% of the infected cell monolayer showed cytopathic effect (CPE), the supernatant containing NiV was harvested and centrifuged at 800 × g for 5 min to remove all residual cells. The supernatant was aliquoted, stored at -80°C and used as virus inoculum in subsequent experiments.

NiV titration

The titer of NiV supernates was determined by virus plaque assay using Vero cells. Briefly, Vero cells were seeded in 24-well tissue culture plates at a concentration of 5×10^5 cells per well and incubated at 37°C overnight. A tenfold serial dilution of NiV inoculum was

prepared with serum-free medium, 200 µL of each dilution was added to Vero cells and pre-adsorbed for 1 h at 37°C. The virus inoculum was then removed, cells were rinsed with serum-free medium and overlaid with a layer of 1.5% carboxymethylcellulose in EMEM supplemented with 2% FBS. The infected cells were fixed with 4% paraformaldehyde on day 3 post infection (PI) and stained with 1% crystal violet. The plaques were counted using a stereomicroscope (Nikon SMZ1000, Japan). The titer of infectious virus was determined and expressed as plaque-forming units per mL (PFU/mL).

NiV infection of cells

NiV infection was performed in IDE8 tick cells and Vero cells. Briefly, IDE8 tick cells were seeded at a concentration of 1×10^6 cells in a flat-sided tube and incubated overnight at 28°C. The tick cells were infected with NiV inoculum at a multiplicity of infection (MOI) of 0.5. The mock-infected tick cells were given mock inoculum (medium) in parallel. After pre-adsorption at 28°C for 1 h, the cells were rinsed thrice with serum-free medium and replenished with fresh L-15B supplemented with 2% FBS. NiV-infected tick cells were examined daily for morphological changes and sampled at 8, 24, 48, 96, 168 and 240 h PI for immunofluorescence microscopy and extraction of viral RNA. IDE8 tick cells were detached by pipetting using a 1 mL micropipettor to direct a stream of medium at the cell layer. The detached cells were pelleted by centrifugation at 200 × g and resuspended in complete L-15B for subsequent experiments. All of the experiments were performed three times with three replicates each.

Vero cells seeded at 1×10^6 cells per well in 12-well plates were infected with NiV inoculum at MOI of 0.5 or with mock inoculum. Pre-adsorption was performed at 37°C for 1 h, followed by rinsing three times with serum-free medium, and then adding fresh EMEM

supplemented with 2% FBS. The NiV-infected Vero cells were examined daily and harvested at 8, 12, 24, 48 and 72 h PI for immunofluorescence microscopy and extraction of viral RNA.

Immunofluorescence microscopy

The NiV-infected IDE8 tick cells and Vero cells were placed onto glass slides coated with poly-L-lysine and fixed with 4% PFA overnight at 4°C. The cells were then rinsed three times with PBS, followed by permeabilisation with 0.5% Igepal (Sigma-Aldrich, USA) in PBS for 30 min. The slides were rinsed with PBS and blocked for 30 min with 3% bovine serum albumin (BSA) in PBS. NiV nucleoprotein (N) was detected using rNiV-N monoclonal antibody (Yong *et al.*, 2020) as primary antibody at a dilution of 1:100, and Alexa Fluor® 594 goat anti-mouse IgG (Invitrogen, USA) as secondary antibody, diluted 1:500. The slides were incubated for 60 min and followed by washing with PBS for 20 min. Next, the cell nuclei were counterstained with Invitrogen™ Hoechst 33342 (Thermo Fisher Scientific, USA) for 10 min. The slides were then rinsed three times with PBS, and excess PBS solution was removed. ProLong™ Gold Antifade Mountant (Thermo Fisher Scientific, USA) was applied and a coverslip was placed over the cells. The fluorescent-stained cells were viewed using a fluorescence microscope (Nikon Eclipse TE-2000E, Japan).

Electron microscopy (EM)

The NiV-infected IDE8 tick cells and Vero cells were harvested at 48, 96 and 240 h PI by centrifugation. Cell pellets were fixed with 4% glutaraldehyde in 0.1 M sodium cacodylate buffer overnight, followed by post-fixing in 1% buffered osmium tetroxide for 2 h, and then cacodylate buffer overnight. The fixed cell pellets were dehydrated in ethanol with increasing concentrations at 35%, 50%, 70%, 95% and three times in 100% ethanol for 15 min each.

The cell pellets were washed twice with propylene oxide for 15 min each, and a final wash with a mixture of propylene oxide and epoxy resin [1 mL Agar-100, 0.6 mL dodecenylsuccinic anhydride (DDSA), 0.6 mL methyl nadic anhydride and 0.05 mL benzyldimethylamine (BDMA)], first at 1:1 for 1 h, followed by 3:1 for 2 h. The cell pellets were then embedded in 100% epoxy resin overnight and polymerised at 60°C the next day. Semi-thin sections were cut and stained with toluidine blue, washed with 95% alcohol, then in water and dried for examination under a light microscope to determine areas of interest. Thin sections were mounted on a 200 mesh copper grid (Ted Pella Inc., USA) and stained with 4% uranyl acetate and Reynold's lead citrate for 5 and 10 min, respectively. The stained grids were washed several times with deionised water and dried on clean filter paper. Ultrastructural changes in NiV-infected IDE8 tick cells and Vero cells were examined using HT7700 transmission electron microscope (Hitachi, Japan).

Immunogold electron microscopy (IEM)

The grids were heated at 95°C in antigen retrieval citrate buffer (Sigma-Aldrich, USA) diluted in 0.01 M PBS, pH 6.0 (Brorson & Nguyen, 2001). The grids were then washed 10 times with PBS containing 0.1% Tween-20 (PBST) for 2 min each, followed by blocking with 10% BSA (diluted in PBS, pH 7.2) for 4 h at 4°C. Incubation with rNiV-N monoclonal antibody (Yong *et al.*, 2020) as primary antibody at a dilution of 1:100 in 10% BSA/PBST was performed overnight at 4 °C. The grids were washed 10 times with PBST for 2 min each again, after which the grids were incubated with goat anti-mouse IgG conjugated with 10 nm gold particles (BBI Solutions, UK) as secondary antibody at a dilution of 1:50 in 3% BSA/PBST for 75 min at room temperature. The grids were washed with PBST and then stained with 4% uranyl acetate and Reynold's lead citrate for 5 min and 10 min, respectively.

155 The stained grids were rinsed several times with deionised H_2O, and dried on clean filter
156 paper. Grids with sections from mock-infected cell cultures were used as negative controls.
157 Ultrastructural changes in NiV-infected IDE8 tick cells and Vero cells were examined using
158 HT7700 transmission electron microscope (Hitachi, Japan).

159

160 **RT-PCR and qRT-PCR**

161 Viral RNA was extracted from the NiV-infected cells using TRI Reagent® (Molecular
162 Research Center, Inc., USA) for detection of NiV RNA by RT-PCR (Chang *et al.*, 2006).
163 Viral RNA was also extracted to determine viral replication in the NiV-infected cell culture
164 supernatant, and RNA extraction was performed using TRI Reagent® LS (Molecular
165 Research Center, Inc., USA). The RNA pellet was dissolved in nuclease-free water and the
166 RNA quality was checked using a NanoPhotometer® P 300 (Implen GmbH, Germany). The
167 NiV N gene or gene copy number was determined by qRT-PCR as previously described
168 (Tiong *et al.*, 2018). Briefly, 1 µL of extracted RNA was added to a final reaction volume of
169 12 µL, containing 3 µL of TaqMan® Fast Virus 1-Step Master Mix (4×), 0.6 µL of
170 TaqMan® Gene Expression assay (20×) and 7.4 µL of nuclease-free water. The forward
171 primer (5'-ATC GGA AAC TAT GTC GAG GAA ACT G-3'), reverse primer (5'-CTC CAA
172 CCC GAA TCT GAT GGT-3'), and fluorescent probe (5'-ATG GCA GGA TTC TTC G-3')
173 were used. A standard curve was made using a 10-fold serial dilution of the NiV RNA
174 standard of known copy number, ranging from 10^1 to 10^6 RNA copies. The qRT-PCR was
175 performed using the StepOnePlus^{TM} instrument (Applied Biosystems, USA) with the
176 following conditions: 50°C for 5 min and 95°C for 20 s, followed by 40 cycles of
177 amplification (95°C for 3 s and 60°C for 30 s). All controls, standards, and samples were
178 performed in triplicate and repeated three times.

179

180 **Statistical analysis**

181 The Independent T test and Levene's test for equality of variances were used to determine
182 whether or not two independent samples were significantly different.

183

184 **RESULTS**

185 **NiV infection and immunofluorescence microscopy**

186 Cells of the *I. scapularis* tick cell line IDE8 were infected with NiV at a MOI of 0.5 and
187 examined at 8, 24, 48, 96, 168 and 240 h PI for CPE by phase-contrast light microscopy.
188 Mock-infected IDE8 tick cells were a mixed population consisting of a well-attached
189 monolayer of cells and clumps of loosely-attached round cells (Figure 1A). NiV-infected
190 IDE8 tick cells appeared similar to mock-infected cells with no obvious evidence of CPE up
191 to the end of the 240 h PI infection period (Figure 1B). Susceptible mammalian Vero cells
192 were prepared in parallel and infected with NiV at MOI 0.5. Mock-infected Vero cells were
193 used as control (Figure 1C). Evidence of CPE was observed in NiV-infected Vero cells at 24
194 h PI (Figure 1D), specifically giant multinucleated cells that increased in number and size
195 with time, and at 72 h PI (Figure 1E) most cells had started to detach from the culture vessel.
196 The presence of viral RNA was confirmed by RT-PCR detection of NiV N gene in the
197 infected IDE8 and Vero cells (data not shown).

198 To confirm that IDE8 tick cells and Vero cells were infected with NiV, cells were
199 examined for the presence of NiV N by immunofluorescence microscopy (Figure 2). Despite
200 the absence of CPE in NiV-infected IDE8 tick cells, NiV N was detected and visualised as a
201 red fluorescence signal using rNiV-N monoclonal antibody and Alexa Fluor® 594
202 conjugated secondary antibody (Figure 2D). The red fluorescent signal was observed in the

cytoplasm of some cells in the culture of NiV-infected IDE8 at 24 h PI. The fluorescent signal was maintained over the following week and was present up to 240 h PI (Figure 2F). In marked contrast to IDE8 tick cells, the fluorescent signal was prominent in the cytoplasm of almost all NiV-infected Vero cells at 72 h PI (Figure 2H). In addition, a highly intense speckled red fluorescent signal was concentrated in certain areas of the cells. These results indicated that the NiV N antigen was present in both infected IDE8 tick cells and Vero cells. No detectable fluorescent signal was observed in negative controls, either the mock-infected IDE8 or Vero cells (Figure 2B and Figure 2G).

Electron microscopy and IEM

Electron microscopy revealed presence of bodies of electron-dense material, similar to previously-described nucleocapsid inclusion bodies (NCI) (Goldsmith *et al.*, 2003) in the cytoplasm of NiV-infected IDE8 tick cells at 96 h (Figure 3A) and 240 h PI (Figure 3B and Figure 3C). NCIs were distinguishable and located in the cytoplasm of NiV-infected IDE8 tick cells. IEM labeling using rNiV-N monoclonal antibody revealed gold particles on structures, ~20 nm wide, representing the herringbone-like appearance typical of paramyxovirus nucleocapsids (Figure 3D). The gold particles were also occasionally evident on the darkened plasma membrane, associated with putative viral budding (Figure 3E and Figure 3F). Closed ring-like structures, 27-33 nm in diameter, were found in NiV-infected IDE8 tick cells (Figure 3G), as well as positive control NiV-infected Vero cells (Figure 3H). None of the above-mentioned ultrastructural features or IEM labelling was observed in mock-infected IDE8 or Vero cells.

Kinetics of NiV replication in cell cultures

To determine the growth characteristics of NiV in IDE8 tick cells, samples of NiV-infected IDE8 cell supernatant were harvested at selected time-points PI and extracellular viral RNA was determined by qRT-PCR of the NiV N gene. The extracellular NiV RNA increased gradually from 35.1 ± 20.9 viral copies/µL at 8 h PI to 162.5 ± 86.2 viral copies/µL at 240 h PI (Figure 4A), and the increase was statistically significant ($p<0.05$). For NiV-infected Vero cells, the increase in extracellular viral RNA was rapid and reached $3.8 \times 10^4 \pm 1.4 \times 10^4$ viral copies/µL at 48 h PI (Figure 4B). This amount was significantly higher than that for NiV-infected IDE8 tick cells ($p<0.05$). Furthermore, the infectivity of NiV released from infected IDE8 tick cells was tested using virus plaque assay on Vero cells. The release of viable and infectious virions from NiV-infected IDE8 tick cells was shown by a gradual increase in the number of PFU obtained during the 240 h sampling period (Table 1). Virus production in NiV-infected IDE8 tick cells at 240 h PI was 15 ± 5.3 PFU/mL as compared to $2.5 \times 10^5 \pm 3.0 \times 10^4$ PFU/mL for NiV-infected Vero cells at 48 h PI. The increase in virion numbers in individual IDE8 cultures, as determined by plaque assay, ranged from 3.3-fold to 12-fold over the 10-day observation period. The trend of NiV virion release at 48 h PI was significantly slower in IDE8 tick cells compared to Vero cells ($p<0.05$).

DISCUSSION

NiV caused a disease outbreak in Malaysia in 1999 that led to at least 265 cases of NiV-infected patients with 105 deaths due to encephalitis (Chua *et al.*, 2000). Several NiV cases were reported after the initial outbreak as cases of relapse and late-onset encephalitis (Tan *et al.*, 2002; Abdullah *et al.*, 2012). In Malaysia, swine were identified as the intermediate and amplifying hosts of NiV (Chua *et al.*, 2000; Chua, 2003). The virus was then transmitted to humans via aerosol droplets. In the Philippines, an epidemiological report identified horses as the intermediate host for transmission of NiV to humans (Ching *et al.*, 2015). Other local

252 domestic animals including goats, pigs and cattle were found to be seropositive for NiV in
253 Bangladesh, where NiV outbreaks occur almost annually (Luby *et al.*, 2009a, 2009b).
254 However, NiV patients in Bangladesh were infected primarily through direct contact via
255 consumption of half-eaten fruit or date palm sap contaminated by bats or their
256 secretions/excretions, without the involvement of an intermediate host. The pteropid fruit bats
257 have been identified as the natural reservoir host for NiV based on various serological
258 findings and surveillance programs, specifically the detection of NiV RNA and NiV
259 seropositivity in bats in Southeast Asia (Yob *et al.*, 2001; Chua *et al.*, 2002; Olson *et al.*,
260 2002; Rahman *et al.*, 2010; Hasebe *et al.*, 2012; Sendow *et al.*, 2013; Wacharapluesadee *et*
261 *al.*, 2021). As pteropid bats have a wide geographical distribution, a spillover of NiV from its
262 natural reservoir host to susceptible hosts could occur, potentially leading to outbreaks in the
263 region and its surroundings.

264 Australian paralysis ticks were suggested to play a role in transmitting HeV (a close
265 relative of NiV) from its natural reservoir, pteropid bats, to horses in Queensland, Australia
266 (Barker, 2003), although experimental evidence was lacking. Consequently, we postulated
267 that ticks could be potential vectors transmitting NiV from bats to other susceptible hosts, as
268 NiV and HeV are closely related molecularly and phylogenetically (Wang *et al.*, 2001). As a
269 first step to test this hypothesis, the IDE8 tick cells were examined to ascertain if NiV could
270 infect and replicate in tick cells.

271 We detected the presence of NiV N antigen in NiV-infected IDE8 tick cells by
272 immunofluorescence, in which the intensity of the fluorescence signal increased with time.
273 Ultrastructural features of NiV-infected IDE8 tick cells were generally similar to those
274 described for NiV-infected Vero cells (Hyatt *et al.*, 2001; Goldsmith *et al.*, 2003), such as
275 electron-dense inclusion bodies in the cytoplasm and darkened plasma membrane associated
276 with viral budding. The closed ring-like structure observed in IEM preparations of NiV-

277 infected IDE8 tick cells and Vero cells, with some similarity to structures previously reported
278 in NiV-infected Vero cells (Goldsmith *et al.*, 2003) was notable. The NiV-infected IDE8 tick
279 cells were able to sustain the infection with no visible cell damage or destruction over a 10-
280 day period. Despite the absence of CPE in NiV-infected IDE8 tick cells, the presence of viral
281 RNA was confirmed by RT-PCR detection of NiV N gene in the infected cells. NiV
282 replication in IDE8 tick cells, measured by extracellular NiV RNA level, was also
283 determined, and the RNA level was lower compared to NiV-infected Vero cells. The pattern
284 of NiV replication kinetics in Vero cells obtained in the present study was found to be
285 consistent with previous reports (Guillaume *et al.*, 2004; Chang *et al.*, 2006), with syncytia
286 formation as characteristic CPE detected as early as 24 h PI, and a rapid increase in viral
287 RNA detected between 12 and 48 h PI. Nonetheless, infectious virus particles were recovered
288 from NiV-infected IDE8 tick cells, although at significantly lower levels than from NiV-
289 infected Vero cells. Absence of CPE, and generally slower rate and lower levels of NiV
290 replication in tick cells compared to mammalian cells are typical of virus infections in tick
291 cell cultures (Rehacek, 1965; Schrauf *et al.*, 2009; Bell-Sakyi *et al.*, 2012; Offerdahl *et al.*,
292 2012; Salata *et al.*, 2018). Further experiments, in which the NiV-infected IDE8 cells are
293 maintained and sampled over a longer period, and/or NiV is passaged repeatedly through
294 IDE8 cells, would reveal whether the virus is able to attain higher titers and adapt to
295 prolonged maintenance in tick cells.

296 Our findings suggest that NiV replicates in IDE8 tick cells, although at a lower level
297 than in mammalian cells, thus providing evidence to support the previously proposed
298 hypothesis that ticks could harbour henipaviruses (Barker, 2003). The reasons for the
299 differences between NiV infection in tick cells and Vero cells remain to be determined.
300 Factors such as different host cell receptors for virus attachment, or different mechanisms of
301 virus entry, could affect virus infectivity. NiV uses ephrin-B2 and -B3 to enter mammalian

cells (Bonaparte *et al.*, 2005; Negrete *et al.*, 2006). Genes encoding putative Eph receptor tyrosine kinase and a putative ephrin fragment are present in the *I. scapularis* genome (Vectorbase, 2022); however, further studies are needed to determine whether NiV entry into tick cells is mediated by ephrin, another ligand, or occurs through phagocytosis. It would be worthwhile to screen for NiV infection in ticks *in vivo* to confirm their possible role as hosts or vectors, although paramyxoviruses have not yet been detected in ticks, likely because of the limited tick virome studies carried out to date, especially in Southeast Asia. Our findings are the first to provide evidence and open new perspectives to a possible alternative route of transmission for NiV from its natural reservoir host, pteropid bats, to other susceptible hosts via ticks, particularly in areas where NiV infection in bats is endemic, but almost no information is available on the incidence of viral infection in susceptible hosts, including humans.

ACKNOWLEDGMENTS

This work was supported in parts by the Malaysia Ministry of Higher Education Exploratory Research Grant Scheme (ERGS/1/11/SKK/UM/3/3), Universiti Malaya Research Grant (UMRG RP013-2012D), Universiti Malaya Postgraduate Research Grant (PG041-2014B), Universiti Malaya Partnership Grant (MG007-2021) and the United Kingdom Biotechnology and Biological Sciences Research Council grants BB/P024270/1 and BB/P024378/1. The IDE8 tick cells were provided by the Tick Cell Biobank and used by kind permission of Ulrike Munderloh, University of Minnesota.

Conflict of interest

The authors declare that they have no conflict of interests.

REFERENCES

Abdullah, S., Chang, L.Y., Rahmat, K., Goh, K.J., Tan, C.T. (2012). Late-onset Nipah virus encephalitis 11 years after the initial outbreak: A case report. *Neurology Asia* **17**: 71-74.

AbuBakar, S., Chang, L.Y., Ali, A.R., Sharifah, S.H., Yusoff, K., Zamrod, Z. (2004). Isolation and molecular identification of Nipah virus from pigs. *Emerging Infecttious Diseases* **10**: 2228-2230. https://doi.org/10.3201/eid1012.040452

Amal, N.M., Lye, M.S., Ksiazek, T.G., Kitsutani, P.D., Hanjeet, K.S., Kamaluddin, M.A., Ong, F., Devi, S., Stockton, P.C., Ghazali, O., Zainab, R. *et al.* (2000). Risk factors for Nipah virus transmission, Port Dickson, Negeri Sembilan, Malaysia: results from a hospital-based case-control study. *Southeast Asian Journal of Tropical Medicine and Public Health* **31**: 301-306.

Arunkumar, G., Chandini, R., Mourya, D.T., Singh, S.K., Sadanandan, R., Sudan, P., Bhargava, B., Nipah Investigators People and Health Study Group. (2019). Outbreak investigation of Nipah virus disease in Kerala, India, 2018. *Journal of Infectious Diseases* **219**: 1867-1878. https://doi.org/10.1093/infdis/jiy612

Barker, S.C. (2003). The Australian paralysis tick may be the missing link in the transmission of Hendra virus from bats to horses to humans. *Medical Hypotheses* **60:** 481-483. https://doi.org/10.1016/s0306-9877(02)00377-8

Bell-Sakyi, L., Kohl, A., Bente, D.A., Fazakerley, J.K. (2012). Tick cell lines for study of Crimean-Congo hemorrhagic fever virus and other arboviruses. *Vector-Borne and Zoonotic Diseases* **12**: 769-781. https://doi.org/10.1089/vbz.2011.0766

Bonaparte, M.I., Dimitrov, A.S., Bossart, K.N., Broder, C.C. (2005). Ephrin-B2 ligand is a functional receptor for Hendra virus and Nipah virus. *Proceedings of the National Academy of Sciences of the United States of America* **102**: 10652-10657. https://doi.org/10.1073/pnas.0504887102

Brorson, S.H. & Nguyen, G.H. (2001). Increased level of immunogold labeling of epoxy sections by rising the temperature significantly beyond 95°C in the antigen retrieval medium. *Micron* **32**: 591-597. https://doi.org/10.1016/s0968-4328(00)00052-4

Chadha, M.S., Comer, J.A., Lowe, L., Rota, P.A., Rollin, P.E., Bellini, W.J., Ksiazek, T.G., Mishra, A. (2006). Nipah virus-associated encephalitis outbreak, Siliguri, India. *Emerging Infectious Diseases* **12**: 235-240. https://doi.org/10.3201/eid1202.051247

Chang, L.Y., Ali, A.R., Hassan, S.S., AbuBakar, S. (2006). Quantitative estimation of Nipah virus replication kinetics in vitro. *Virology Journal* **3**: 47. https://doi.org/10.1186/1743-422X-3-47

Ching, P.K., de los Reyes, V.C., Sucaldito, M.N., Tayag, E., Columna-Vingno, A.B., Malbas, F.F.Jr., Bolo, G.C.Jr., Sejvar, J.J, Eagles, D., Playford, G., Dueger, E. *et al.* (2015). Outbreak of henipavirus infection, Philippines, 2014. *Emerging Infecttious Diseases* **21**: 328-331. https://doi.org/10.3201/eid2102.141433

Chua, K.B., Bellini, W.J., Rota, P.A., Harcourt, B.H., Tamin, A., Lam, S.K., Ksiazek, T.G., Rollin, P.E., Zaki, S.R., Shieh, W., Goldsmith, C.S. *et al.* (2000). Nipah virus: a recently emergent deadly paramyxovirus. *Science* **288**: 1432-1435. https://doi.org/10.1126/science.288.5470.1432

Chua, K.B., Koh, C.L., Hooi, P.S., Wee, K.F., Khong, J.H., Chua, B.H., Chan, Y.P., Lim, M.E., Lam, S.K. (2002). Isolation of Nipah virus from Malaysian Island flying-foxes. *Microbes and Infection* **4**: 145-151. https://doi.org/10.1016/s1286-4579(01)01522-2

Chua, K.B. (2003). Nipah virus outbreak in Malaysia. *Journal of Clinical Virology* **26**: 265-275. https://doi.org/10.1016/s1386-6532(02)00268-8

Field, H., Young, P., Yob, J.M., Mills, J., Hall, L., Mackenzie, J. (2001). The natural history of Hendra and Nipah viruses. *Microbes and Infection* **3**: 307-314. https://doi.org/10.1016/s1286-4579(01)01384-3

Goldsmith, C.S., Whistler, T., Rollin, P.E., Ksiazek, T.G., Rota, P.A., Bellini, W.J., Daszak, P., Wong, K.T., Shieh, W.J., Zaki, S.R. (2003). Elucidation of Nipah virus morphogenesis and replication using ultrastructural and molecular approaches. *Virus Research* **92**: 89-98. https://doi.org/10.1016/s0168-1702(02)00323-4

Guillaume, V., Lefeuvre, A., Faure, C., Marianneau, P., Buckland, R., Lam, S.K., Wild, T.F., Deubel, V. (2004). Specific detection of Nipah virus using real-time RT-PCR (TaqMan). *Journal of Virological Methods* **120**: 229-237. https://doi.org/10.1016/j.jviromet.2004.05.018

Hasebe, F., Thuy, N.T.T., Inoue, S., Yu, F., Kaku, Y., Watanabe, S., Akashi, H., Dat, D.T., Mai, L.T.Q., Morita, K. (2012). Serologic evidence of Nipah virus infection in bats, Vietnam. *Emerging Infectious Diseases* **18**: 536-537. https://doi.org/10.3201/eid1803.111121

Hepojoki, J., Kipar, A., Korzyukov, Y., Bell-Sakyi, L., Vapalahti, O., Hetzel, U. (2015). Replication of boid inclusion body disease-associated arenaviruses is temperature sensitive in both boid and mammalian cells. *Journal of Virology* **89**: 1119-1128. https://doi.org/10.1128/JVI.03119-14

Hsu, V.P., Hossain, M.J., Parashar, U.D., Ali, M.M., Ksiazek, T.G., Kuzmin, I., Niezgoda, M., Rupprecht, C., Bresee, J., Breiman, R.F. (2004). Nipah virus encephalitis reemergence, Bangladesh. *Emerging Infectious Diseases* **10**: 2082-2087. https://doi.org/10.3201/eid1012.040701

Hyatt, A.D., Zaki, S.R., Goldsmith, C.S., Wise, T.G., Hengstberger, S.G. (2001). Ultrastructure of Hendra virus and Nipah virus within cultured cells and host animals. *Microbes and Infection* **3**: 297-306. https://doi.org/10.1016/s1286-4579(01)01383-1

Luby, S.P., Gurley, E.S., Hossain, M.J. (2009a). Transmission of human infection with Nipah virus. *Clinical Infectious Diseases* **49**: 1743-1748. https://doi.org/10.1086/647951

Luby, S.P., Hossain, M.J., Gurley, E.S., Ahmed, B.N., Banu, S., Khan, S.U., Homaira, N., Rota, P.A., Rollin, P.E., Comer, J.A., Kenah, E. *et al.* (2009b). Recurrent zoonotic

transmission of Nipah virus into humans, Bangladesh, 2001-2007. *Emerging Infectious Diseases* **15**: 1229-1235. https://doi.org/10.3201/eid1508.081237

Munderloh, U.G. & Kurtti, T.J. (1989). Formulation of medium for tick cell culture. *Experimental and Applied Acarology* **7**: 219-229. https://doi.org/10.1007/BF01194061

Munderloh, U.G., Liu, Y., Wang, M., Chen, C., Kurtti, T.J. (1994). Establishment, maintenance and description of cell lines from the tick *Ixodes scapularis*. *Journal of Parasitology* **80**: 533-543.

Negrete, O.A., Wolf, M.C., Aguilar, H.C., Enterlein, S., Wang, W., Muhlberger, E., Su, S.V., Bertolotti-Ciarlet, A., Flick, R., Lee, B. (2006). Two key residues in ephrinB3 are critical for its use as an alternative receptor for Nipah virus. *PLoS Pathogen* **2**: e7. https://doi.org/10.1371/journal.ppat.0020007

Nicholson, W.L., Sonenshine, D.E., Noden, B.H., Brown, R.N. (2018). Ticks (Ixodida). In: Medical and Veterinary Entomology, Mullen, G.R. & Durden, L.A. (editors) 3rd edition. Academic Press, pp. 603-672.

Offerdahl, D.K., Dorward, D.W., Hansen, B.T., Bloom, M.E. (2012). A three-dimensional comparison of tick-borne flavivirus infection in mammalian and tick cell lines. *PLoS One* **7**: e47912. https://doi.org/10.1371/journal.pone.0047912

444 Olson, J.G., Rupprecht, C., Rollin, P.E., An, U.S., Niezgoda, M., Clemins, T., Walston, J.,
445 Ksiazek, T.G. (2002). Antibodies to Nipah-like virus in bats (*Pteropus lylei*), Cambodia.
446 *Emerging Infectious Diseases* **8**: 987-988. https://doi.org/10.3201/eid0809.010515

447

448 Parashar, U.D., Sunn, L.M., Ong, F., Mounts, A.W., Arif, M.T., Ksiazek, T.G., Kamaluddin,
449 M.A., Mustafa, A.N., Kaur, H., Ding, L.M., Othman, G. *et al.* (2000). Case-control study of
450 risk factors for human infection with a new zoonotic paramyxovirus, Nipah virus, during a
451 1998-1999 outbreak of severe encephalitis in Malaysia. *Journal of Infectious Diseases* **181**:
452 1755-1759. https://doi.org/10.1086/315457

453

454 Rahman, S.A., Hassan, S.S., Olivial, K.J., Mohamed, M., Chang, L.Y., Hassan, L., Saad,
455 N.M., Shohaimi, A.S., Mamat, Z. ., Naim, M.S., Epstein, J.H. *et al.* (2010). Characterization
456 of Nipah virus from naturally infected *Pteropus vampyrus* bats, Malaysia. *Emerging*
457 *Infectious Diseases* **16**: 1990-1993. https://doi.org/10.3201/eid1612.091790

458

459 Rehacek, J. (1965). Cultivation of different viruses in tick tissue cultures. *Acta Virologica* **9**:
460 332-337.

461

462 Salata, C., Monteil, V., Karlberg, H., Celestino, M., Devignot, S., Leijon, M., Bell-Sakyi, L.,
463 Bergeron, E., Weber, F., Mirazimi, A. (2018). The DEVD motif of Crimean-Congo
464 hemorrhagic fever virus nucleoprotein is essential for viral replication in tick cells. *Emerging*
465 *Microbes & Infections* **7**: 190. https://doi.org/10.1038/s41426-018-0192-0

466

Schrauf, S., Mandl, C.W., Bell-Sakyi, L., Skern, T. (2009). Extension of flavivirus protein C differentially affects early RNA synthesis and growth in mammalian and arthropod host cells. *Journal of Virology* **83**: 11201-11210. https://doi.org/10.1128/JVI.01025-09

Sendow, I., Ratnawati, A., Taylor, T., Adjid R.M.A., Saepulloh, M., Barr, J., Wong, F., Daniels, P., Field, H. (2013). Nipah virus in fruit bat *Pteropus vampyrus* in Sumatera, Indonesia. *PLoS One* **8**: e69544. https://doi.org/10.1371/journal.pone.0069544

Tan, C.T., Goh, K.J., Wong, K.T., Sarji, S.A., Chua, K.B., Chew, N.K., Murugasu, P., Loh, Y.L., Chong, H.T., Tan, K.S., Thayaparan, T. *et al.* (2002). Relapsed and late-onset Nipah encephalitis. *Annals of Neurology* **51**: 703-708. https://doi.org/10.1002/ana.10212

Tiong, V., Shu, M.H., Wong, W.F., AbuBakar, S., Chang, L.Y. (2018). Nipah virus infection of immature dendritic cells increases its transendothelial migration across human brain microvascular endothelial cells. *Frontiers in Microbiology* **9**: 2747. https://doi.org/10.3389/fmicb.2018.02747

Vectorbase (2022). Data set: *Ixodes scapularis* Wikel genome sequence and annotation. https://vectorbase.org/ Accessed 25 August 2022.

Wacharapluesadee, S., Ghai, S., Duengkae, P., Manee-Orn, P., Tranapongtharm, W., Saraya, A.W., Yingsakmongkon, S., Joyjinda, Y., Suradhat, S., Ampoot, W., Nuansrichay, B. *et al.* (2021). Two decades of one health surveillance of Nipah virus in Thailand. *One Health Outlook* **3**: 12. https://doi.org/10.1186/s42522-021-00044-9

Wang, L., Harcourt, B.H., Yu, M., Tamin, A., Rota, P.A., Bellini, W.J., Eaton, B.T. (2001). Molecular biology of Hendra and Nipah viruses. *Microbes and Infection* **3**: 279-287. https://doi.org/10.1016/s1286-4579(01)01381-8

Yadav, P.D., Sahay, R.R., Balakrishnan, A., Mohandas, S., Radhakrishnan, C., Gokhale, M.D., Balasubramanian, R., Abraham, P., Gupta, N., Sugunan, A.P., Khobragade, R. *et al.* (2022). Nipah virus outbreak in Kerala state, India amidst of COVID-19 pandemic. *Frontiers in Public Health* **10**: 818545. https://doi.org/10.3389/fpubh.2022.818545

Yob, J.M., Field, H., Rashdi, A.M., Morrissy, C., van der Heide, B., Rota, P., bin Adzhar, A., White, J., Daniels, P., Jamaluddin, A., Ksiazek, T. (2001). Nipah virus infection in bats (order Chiroptera) in peninsular Malaysia. *Emerging Infectious Diseases* **7**: 439-441. https://doi.org/10.3201/eid0703.010312

Yong, M.Y., Lee, S.C., Ngui, R., Lim, Y.A.L., Phipps, M.E., Chang, L.Y. (2020). Seroprevalence of Nipah virus infection in Peninsular Malaysia. *Journal of Infectious Diseases* **221(Suppl 4)**: S370-S374. https://doi.org/10.1093/infdis/jiaa085

Figure legends

Figure 1. Phase contrast light microscopic examination of IDE8 tick cells and Vero cells infected with Nipah virus (NiV) at MOI of 0.5. (A) Mock-infected IDE8 tick cells as negative control, (B) NiV-infected IDE8 tick cells at 240 h following infection, (C) Mock-infected Vero cells as negative control, (D) NiV-infected Vero cells at 24 h, (E) NiV-infected Vero cells at 72 h. All images were taken at 200× magnification by inverted light microscope; scale bars = 1 μm.

Figure 2. Immunofluorescence microscopy analysis of IDE8 tick cells and Vero cells following infection with Nipah virus (NiV). Presence of NiV in the infected cells was detected using rNiV-N monoclonal antibody and Alexa Fluor® 594 goat anti-mouse IgG, and appeared red. (A) and (B) Mock-infected IDE8 tick cells as negative control, (C) and (D) NiV-infected IDE8 tick cells at 24 h PI, (E) and (F) NiV-infected IDE8 tick cells at 240 h PI, (G) Mock-infected Vero cells as negative control, (H) NiV-infected Vero cells at 72 h PI. The cellular nucleus was counterstained with Hoechst 33342 stain, and appeared blue. All images were taken at 400× magnification by phase-contrast and fluorescent microscope; scale bars = 1 μm.

Figure 3. Transmission electron micrographs of IDE8 tick cells and Vero cells infected with Nipah virus (NiV). Electron-dense material, similar to that previously described as nucleocapsid inclusion bodies (NCI) in the cytoplasm of NiV-infected IDE8 tick cells (A) at 96 h PI when dense material occupied part of the cytoplasm (arrow); scale bar 2000 nm, (B) at 240 h PI, when dense material almost completely filled the cytoplasm (arrow); scale bar 2000 nm, (C) a NCI (arrow) at 240h PI; scale bar 200 nm, (D) immuno-electron micrograph showing typical herringbone structure (arrow) associated with paramyxoviruses in the cytoplasm at 96 h PI, with gold particles targeting the NiV nucleoprotein (N) attached along the herringbone structure; scale bar 100 nm, (E) gold particles on darkened plasma membrane

(arrow) at 48 h PI; scale bar 100 nm, (F) gold particles present on a putative viral budding structure (arrow) at 48 h PI; scale bar 100 nm, and (G) closed ring-like structures of 27-33 nm diameter (arrows); scale bar 100 nm. (H) Similar ring-like structures were noted in cytoplasm of a NiV-infected Vero cell (arrows); scale bar 100 nm.

Figure 4. Nipah virus **(**NiV) replication kinetics in infected (A) IDE8 tick cells and (B) Vero cells. Extracellular NiV RNA copy numbers were determined using a qRT-PCR targeting the NiV N gene. Data are shown from three experiments each with three biological replicates, error bars represent standard deviation.

Table 1: Plaque assay titration of Nipah virus (NiV) particles in supernate of NiV-infected IDE8 tick cells and Vero cells harvested over 240 h and 48 h periods post infection, respectively (means of three independent experiments with three biological replicates and two technical replicates each).

	Plaque-forming units (PFU)/mL from supernate of NiV-infected IDE8 tick cells		**Plaque-forming units (PFU)/mL from supernate of NiV-infected Vero cells**	
Hours PI	**Mean number of plaques (range)**	**Standard deviation**	**Mean number of plaques (range)**	**Standard deviation**
0	2.5 (2-3)	0.5	1.0 (0-2)	1.2
4	4.3 (3-6)	1.4	2.3 (1-3)	1.0
8	3.5 (2-5)	1.2	4.8 (4-7)	1.5
12	ND	ND	122.5 (100-160)	26.3
24	4.0 (0-8)	3.0	1.7×10^4 ($1.0\text{-}2.1 \times 10^4$)	5.2×10^3
48	4.2 (2-6)	1.8	2.5×10^5 ($2.2\text{-}3.0 \times 10^5$)	3.0×10^4
96	5.5 (4-7)	1.4	ND	ND
168	5.7 (4-9)	1.8	ND	ND
240	15.0 (10-24)	5.3	ND	ND

ND = not done.

548 **Figure 1**

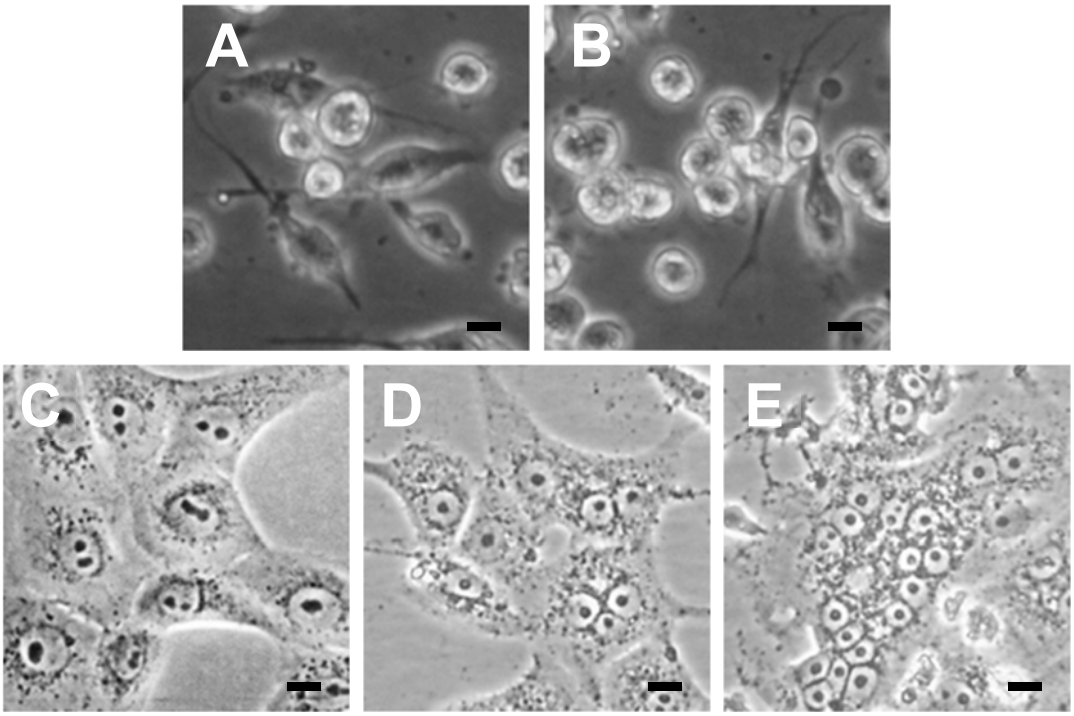

549 **Figure 2**

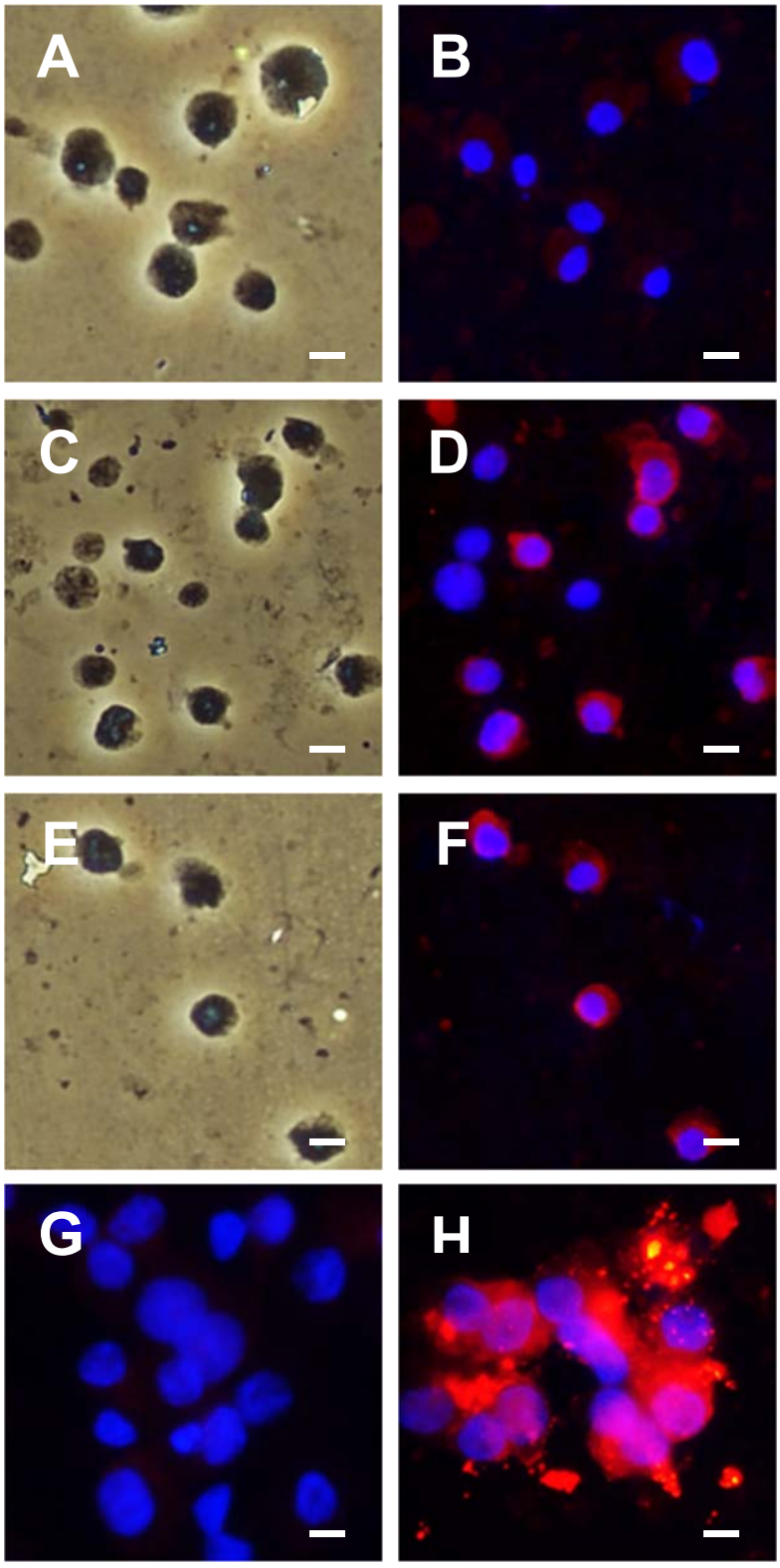

550 **Figure 3**

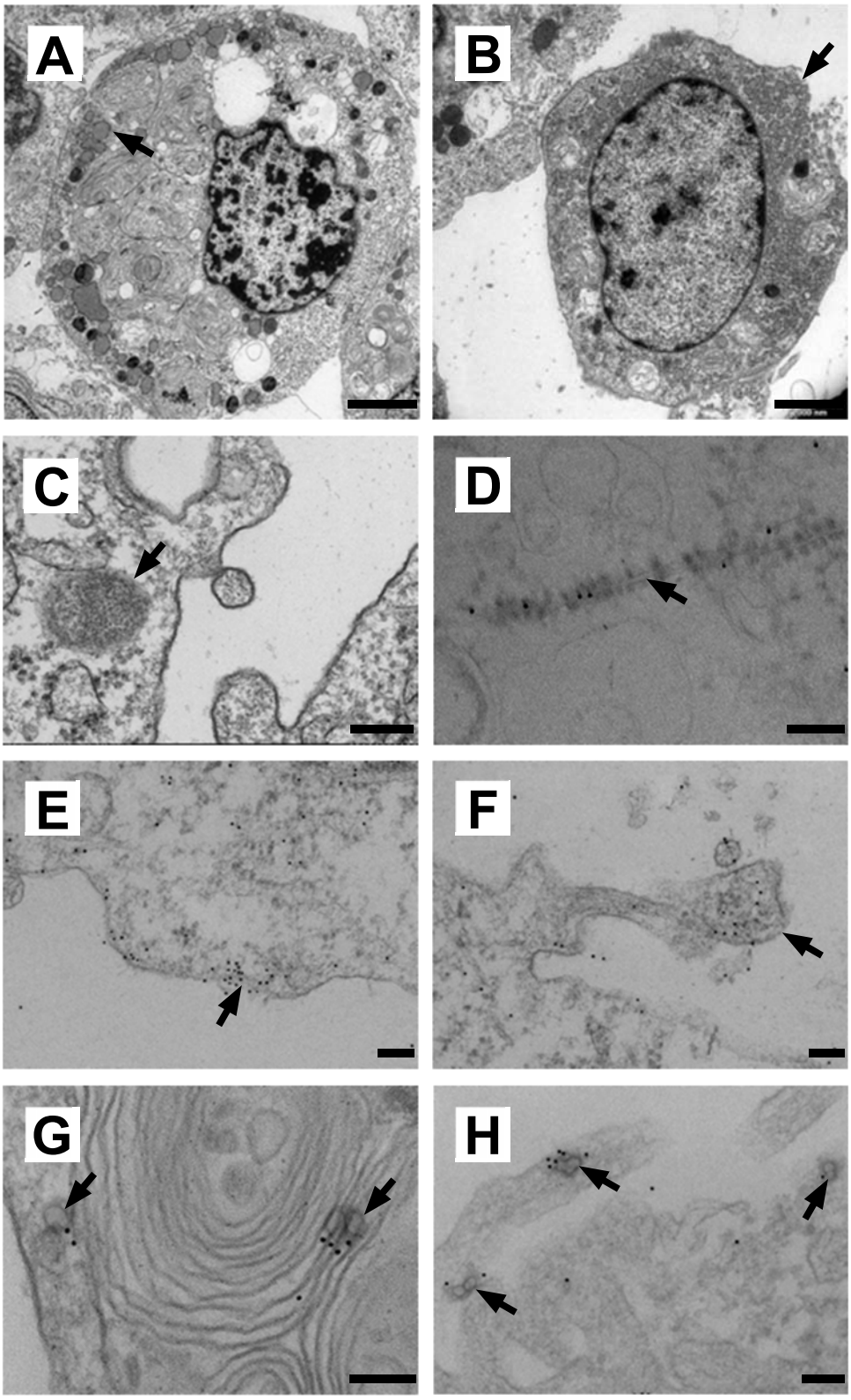

551 **Figure 4**

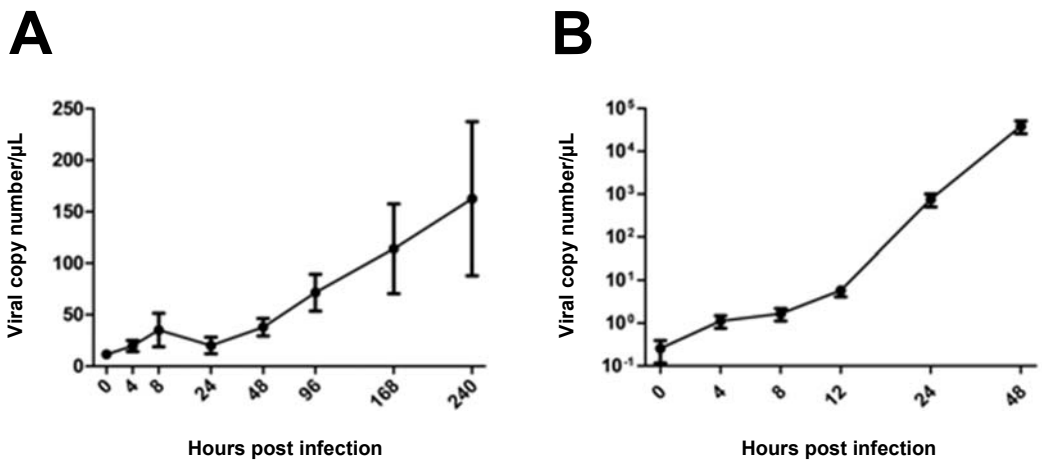
A
B
Viral copy number/µL
250
200
150
100
50
0
0
4
8
24
48
96
168
240
Hours post infection
Viral copy number/µL
10^5
10^4
10^3
10^2
10^1
10^0
10^{-1}
0
4
8
12
24
48
Hours post infection